Hindawi Publishing Corporation
International Journal of Photoenergy
Volume 2016, Article ID 8507625, 9 pages
http://dx.doi.org/10.1155/2016/8507625

*Research Article*

# Simulation on the Performance of Dye Solar Cell Incorporated with $TiO_2$ Passivation Layer

**Unan Yusmaniar Oktiawati,[1] Norani Muti Mohamed,[2,3] and Zainal Arif Burhanudin[1]**

[1]*Electrical and Electronic Engineering Department, Universiti Teknologi PETRONAS, 32610 Seri Iskandar, Perak, Malaysia*
[2]*Centre of Innovative Nanostructures & Nanodevices (COINN), Universiti Teknologi PETRONAS, 32610 Seri Iskandar, Perak, Malaysia*
[3]*Fundamental & Applied Sciences Department, Universiti Teknologi PETRONAS, 32610 Seri Iskandar, Perak, Malaysia*

Correspondence should be addressed to Norani Muti Mohamed; noranimuti_mohamed@petronas.com.my

Received 10 December 2015; Accepted 1 March 2016

Academic Editor: Meenakshisundaram Swaminathan



Dye Solar Cell (DSC) has started to gain interest in the recent years for practical application because of its ecofriendly, low cost, and easy fabrication. However, its efficiency is still not as competitive as the conventional silicon based solar cell. One of the research efforts to improve the efficiency of DSC is to use the passivation layer in between the photoelectrode material and the conductive oxide substrate. Thus, the objective of this simulation study is to investigate the effect of passivation layer on the performance of DSC. Properties from literatures which are based on physical work were captured as the input for the simulation using process, ATHENA, and device, ATLAS, simulator. Results have shown that the addition of two-20 nm $TiO_2$ passivation layers on DSC can enhance the efficiency by 11% as the result of less recombination, higher electron mobility, and longer electron lifetime.

## 1. Introduction

Dye Solar Cell (DSC) is the third-generation solar cell that offers ecofriendly, low cost, and easy processing [1]. As shown in Figure 1(a), DSC is made up of photoelectrochemical cell consisting of dye-sensitized $TiO_2$ layer, electrolyte, and platinum (Pt) film in between two transparent conducting oxide (TCO) glasses. The material used for fabricating DSC is abundant and belongs to nontoxic material. The procedure to build the DSC is also simple and easy. But behind all these advantages, there are a number of problems that still need to be addressed in order to realize DSC practically. One of them is its efficiency, which can be described by the following equation:

$$\text{efficiency} = \frac{J_{sc} V_{oc} \text{FF}}{I_s}, \quad (1)$$

where $J_{sc}$ is the short circuit density, $V_{oc}$ is the open circuit voltage, FF is the fill factor, and $I_s$ is the intensity of the incident light.

In the presence of sunlight, the photons strike the dyes with enough energy to create an excited state of the dye, resulting in generating electron which can be injected directly into the conduction band of $TiO_2$ as shown in Figure 1(b). Regeneration process in dye happens when the electrons from the electrolyte are restored. The process is cycled, causing the generation of electricity. In reality, the generated electrons could travel in the reverse direction and recombine with the oxidized dyes [2] before regeneration process takes place. The dynamic competition between the electrons generation and recombination has been found to be the limitation that restricts the development of higher efficiency DSCs. Recombination mainly occurs at the interface between DSC elements such as $TiO_2$/electrolyte and the transparent conducting oxide (TCO)/electrolyte. Recombination may cause significant losses in DSC. In order to improve the performance of DSC, reducing the recombination is essential [3]. It has been reported that the back reaction process of electrons to the electrolyte is more prevalent at the TCO/electrolyte interface than at the photoelectrode film/electrolyte interface.

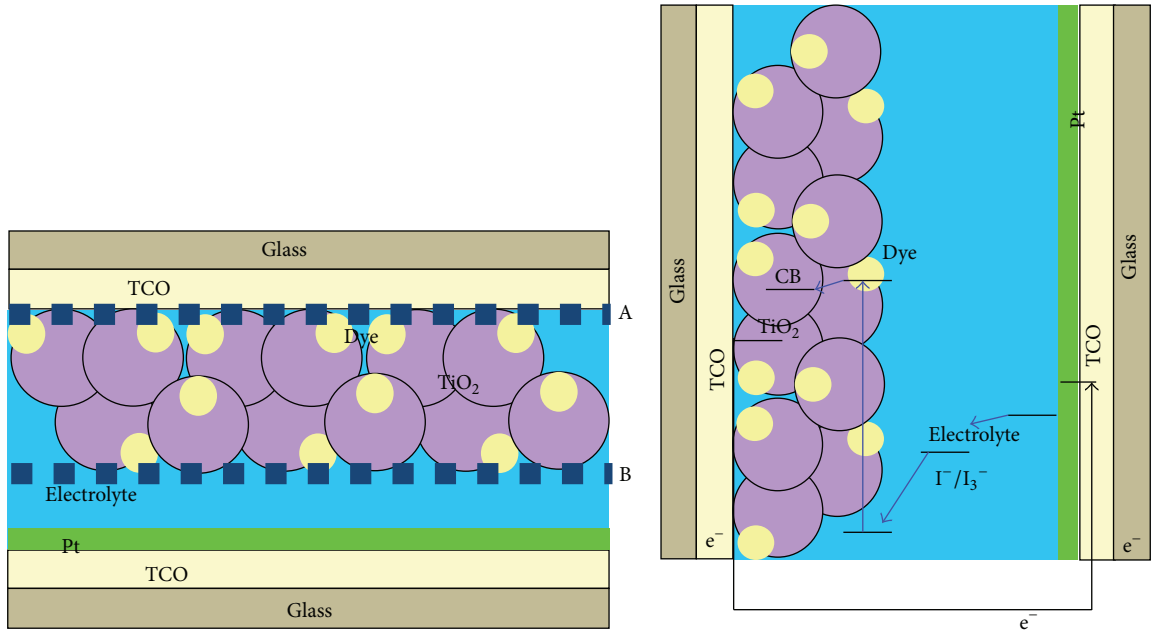


Figure 1: Illustration of DSC. (a) Structure. (b) Electron transport.

This condition highlights the potential of utilizing two thin films of $TiO_2$ layer above (marked as A) and below (marked as B in Figure 1(a)) the photoelectrode $TiO_2$ layer which later proved to have increased the efficiency [4].

One of the methods to be employed to control the recombination process in DSC is through the use of a thin layer at the TCO/electrolyte contacts. This layer is the single $TiO_2$ passivation layer, indicated as A in Figure 1(a). Several works have reported the use of a thin layer of other materials such as ZnO and $Nb_2O_5$ instead of $TiO_2$ between the photoelectrode and the TCO substrate [5–10]. They also reported that adding $TiO_2$ passivation layer may affect the performance as well as the efficiency of DSC.

Adding $TiO_2$ passivation layer is expected to reduce the possibility of recombination on electrolyte/TCO interface. On the other hand, the addition of $TiO_2$ passivation layer can reduce conductivity of electrolyte that will lead to the decrease in short circuit density ($J_{sc}$), as described in (1), as well as the efficiency. Moreover, adding $TiO_2$ passivation layer may result in huge electron trapping in DSC which may reduce the electron lifetime. Thus, striking a balance between these two factors may prove beneficial to the performance of DSC. It is believed that optimizing the thickness of $TiO_2$ passivation layer will improve the efficiency as well as DSC performance.

In order to understand how the presence of $TiO_2$ passivation layer can reduce the recombination process leading to an improvement in DSC performance, one needs to analyze the kinetics of the components within DSC system. If recombination is reduced, more electrons can flow to the cathode, generating more electricity in DSC. Recombination process in DSC may affect recombination rate through

$$U = kn, \tag{2}$$

where $U$ is recombination rate, $k$ is constant of recombination, and $n$ is electron concentration [11]. Changing the amount of electron concentration in DSC will cause a change in the electron lifetime. This is because the electron lifetime is inversely proportional to the recombination rate as described in

$$\tau = \frac{\Delta n}{U}, \tag{3}$$

where $\tau$ is electron lifetime and $\Delta n$ is the change in electron concentration [12]. Thus, smaller recombination rate would mean longer electron lifetime, whilst longer electron lifetime may cause higher $J_{sc}$, leading to higher performance of DSC.

Another parameter related to the recombination is recombination resistance. Electron lifetime affected the recombination resistance through

$$R_{rec} = \frac{kT\tau}{Aq^2nd}, \tag{4}$$

where $T$ is temperature, $A$ is area, $q$ is electron charge, and $d$ is the thickness [13]. The thickness, $d$, is referring to the thickness of the photoelectrode material, namely, $TiO_2$ film. When (3) is equated to (4), it explained the inversely proportional relationship between $U$ and $R_{rec}$. Higher recombination resistance means less occurrence of recombination process in DSC.

Meanwhile, there is also another parameter called transport resistant that is affected by the thickness as shown in

$$R_T = \frac{kTd}{Aq^2nD}, \tag{5}$$

where $D$ is diffusion coefficient [13]. The thicker the layer is, the higher the transport resistance would be. On the other

hand, higher diffusion coefficient will increase the electron mobility as described in

$$D = \frac{kT\mu}{q}, \tag{6}$$

where $\mu$ is electron mobility [14]. From (4), there is the need for a thicker thickness, $d$, of the film in order to increase the transport resistance which can then reduce the recombination process. In DSC system, it would mean a layer of film at the TCO/electrolyte interface where the occurrence of recombination is more severe.

Experimental work by Eskandar et al. showed that adding the passivation layer can improve the performance of DSC [15]. Recombination is reduced as indicated by the higher recombination resistance for DSC with $TiO_2$ passivation layer. Moreover, lower recombination may increase the electron lifetime. It is also confirmed by Waita et al. [16] that electron lifetime in DSC increased as the effect of adding $TiO_2$ passivation layer. Several researchers have successfully improved the performance of DSC by using passivation layer [17–20]. However, another finding [15] showed that $TiO_2$ passivation layer can cause the electrons to be trapped so that they are unable to flow to the cathode, resulting in low $J_{sc}$. Thus, with these contradicting effects, there is the need to optimize the thickness of the $TiO_2$ passivation layer in order to achieve longer electron lifetime with minimal electron trapping and higher diffusion coefficient for faster electron mobility but also lower recombination.

The work here involved simulated analysis on the performance of DSC by adding $TiO_2$ passivation layer of different thickness at the TCO/electrolyte interface and adopting this optimum thickness for the second passivation layer at the $TiO_2$/electrolyte interface. Properties of the components of DSC were extracted from literatures which are based on physical work and were used as the input for the simulated environment. Michael et al. [20] had earlier reported a simulation work on Si-based solar cell using ATLAS by Silvaco. Simulation study allows for prediction of the behavior of the components in the system where, in this case, it can lead to a better understanding of the kinetics within DSC. This can be acquired without running a series of costly experimental works. The predicted behavior based on optimized simulated parameters can then be validated directly using the physical work. Simulation result also provides detail that may not be experimentally measurable using the current technology.

## 2. Simulation Model

ATHENA and ATLAS simulation software by Silvaco were used to simulate DSC performance. ATLAS is a device simulator whilst ATHENA is a group of process simulations. By using this software, virtual fabrication of DSC will be built. ATLAS calculates the electrical parameters by simulating the electron transport on a two-dimensional mesh. It will give the output of extracted electrical characteristics of the simulated model. The most suitable model from several models offered in ATHENA needs to be chosen in order to represent DSC system. In this model, manipulation of material, physical structure, and dimension can be carried out.

ATLAS offers several selections of material models that can be employed in the simulation, namely, mobility, recombination, statistics, impact ionization, tunneling model, energy transport, and heat flow equation [33]. These models can be endorsed for the entire device or the specific region only. Statistic model is about acceptor and donor ion density. Impact ionization is more about electron injection when recombination happened. Tunneling model is more suitable for semiconductor device with occupied tunnel in it. Energy transport is more about energy used for carrier transport. Heat flow equation is used for defining heat flow. Among those categories, mobility and recombination models are the nearby model for DSC simulation in which both processes occurred in DSC.

Mobility models in ATLAS are more suitable for silicon and GaAs based semiconductor device with limited conditions whereas DSC will not be using those materials. Instead, the recombination model was selected since, for DSC, the simulation will focus on recombination process. Since DSC utilized $TiO_2$ that belongs to wide band gap material then SRH (Shockley-Read-Hall) model was adopted as it was more relevant to the recombination process in DSC. The net recombination rate for SRH recombination is given by

$$R_{\mathrm{SRH}} = \frac{np - {n_i}^2}{\tau_n \left(p + n_i\right) + \tau_p \left(n + n_i\right)}, \tag{7}$$

where $n$ is electron density, $p$ is hole density, $n_i$ is electron in intrinsic level, $\tau_n$ and $\tau_p$ are the minority carrier lifetimes for electrons and holes, and it is assumed that the trap level coincides with the intrinsic level [33]. Equation (7) is derived from (2).

As the input for the simulation of DSC here in ATLAS and ATHENA, properties, namely, affinity, energy gap, and permittivity, are extracted from literatures. Affinity is the amount of energy obtained when an electron is moving whereas energy gap is the amount of energy required to excite it whilst permittivity is its ability to store energy. DSC was then designed in ATHENA based on the data properties shown in Table 1. In this simulation, working temperature for DSC is set at 300 K with 1.5 AM full sunlight condition. The electrolyte used is iodine-based electrolyte. To fulfill the need of simulated light source, input of an optical file consisting of *nk* values is extracted from UV/VIS spectroscopy result. This optical file contains the refractive index, $n$, and extinction coefficient, $k$, for dye N719-sensitized $TiO_2$. It is important for the simulation of DSC as it defines the condition of light passing through the DSC.

In this simulation, the input and structure of DSC are shown in Figure 2. DSC is designed in a sandwich-like structure, consisting of a thin layer of metal oxide layer as the passivation layer and $TiO_2$ nanoparticle with absorbed N719 dye, represented by the red region. The electrolyte used is iodine, which is displayed by the green region. The performance in the form of electrical data was extracted for the simulated DSC system and then compared and verified with the results of the closest related experimental work.

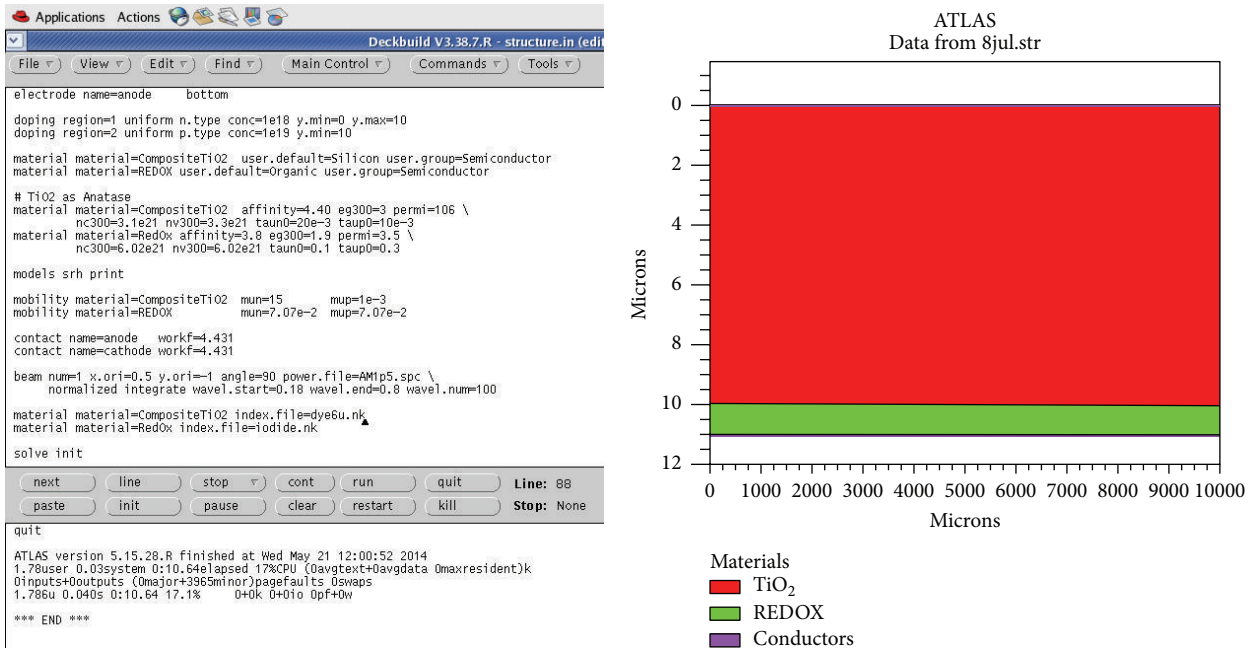


Figure 2: Simulated DSC. (a) Input and (b) structure.

Table 1: Properties of $TiO_2$, $Nb_2O_5$, and ZnO.

| Property | Unit | $TiO_2$ | Ref. | $Nb_2O_5$ | Ref. | ZnO | Ref. |
|---|---|---|---|---|---|---|---|
| Affinity | eV | 4.3 | [23] | 3.35 | [24] | 4.2 | [25] |
| Energy gap | eV | 3.2 | [1] | 3.4 | [26] | 3.37 | [27] |
| Permittivity | F/cm | 46 | [28] | 41 | [29] | 10.4 | [30] |

To investigate the effects of $TiO_2$ passivation layer, simulations of DSC without any passivation layer and also with $TiO_2$ passivation layer in DSC as illustrated in Figure 1(a) are compiled. Simulations have the same structure as shown in Figure 2. Properties of $TiO_2$ used as photoanode and passivation layer are shown in Table 1.

In DSC, electron will be injected from the dye to $TiO_2$ photoanode. Then, electron will travel to the cathode through passivation layer. In order to get higher electron injection, the conduction band (CB) of material used as the passivation layer needs to be closer to the CB of $TiO_2$, which is the photoanode. As shown in Figure 3, CB of $TiO_2$, $Nb_2O_5$, and ZnO are located below the CB of N719 dye. It means that those materials can be used as the passivation layer. So as to comprehend the effects of material used as the passivation layer, simulations are conducted by adjusting the properties of material used as passivation layer. Simulation with the same structure as shown in Figure 2 is conducted and compared with simulation which has different material of additional layer as passivation layer, namely, $TiO_2$, $Nb_2O_5$, and ZnO. Properties of materials used as passivation layer are shown in Table 1.

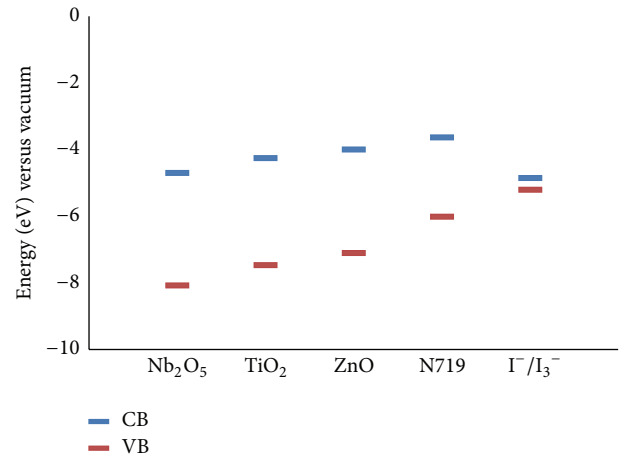


Figure 3: Energy band diagram [21, 22].

By varying the thickness of $TiO_2$ passivation layer, simulations are also compiled to study the effects of thickness of $TiO_2$ passivation layer. $TiO_2$ passivation layer is varied with its thickness from 10, 20, and 50 to 100 nm. Properties of $TiO_2$ used as photoanode and passivation layer are as shown in Table 1. Structure used in simulation is as shown in Figure 2. Simulated results obtained are compared with the experimental result which has the closest condition to the simulated DSC. Lastly, DSC is simulated with two-20 nm thick $TiO_2$ passivation layers with position as shown as A and B in Figure 1.

To measure the accuracy of simulation, calculation of error is also conducted based on

$$e_R = \frac{\left|R_{\text{exp}} - R_{\text{sim}}\right|}{R_{\text{exp}}} * 100\%,$$

$$\text{RMSE} = \sqrt{\frac{\sum |e_R|^2}{N}}, \quad (8)$$

$$\text{MBE} = \frac{\sum e_R}{N},$$

$$\text{MAE} = \frac{\sum |e_R|}{N}.$$

## 3. Results and Discussion

*3.1. Effects of Passivation Layer.* By adding $TiO_2$ passivation layer, the thickness of $TiO_2$ photoelectrode will increase. As shown in (4), there is an inversely proportional relationship between $R_{\text{rec}}$ and thickness, $d$. $R_{\text{rec}}$ is higher for simulated DSC without any additional passivation layer compared to $R_{\text{rec}}$ for simulated DSC with additional $TiO_2$ passivation layer. This implies that recombination is easily occurring in simulated DSC without any additional passivation layer compared to the one with the additional $TiO_2$ passivation layer.

Meanwhile, there is proportional relation between $R_T$ and thickness as shown by (5). $R_T$ is lower for simulated DSC with additional $TiO_2$ layer as passivation layer compared to $R_T$ for simulated DSC without any additional passivation layer.

It means that electron transport is easier in simulated DSC with additional $TiO_2$ layer as passivation layer compared to electron in simulated DSC without any additional passivation layer. This condition indicates that the charge transfer remains more efficient and results in higher $J_{\text{sc}}$ in simulated DSC with additional $TiO_2$ layer as passivation layer compared to that in simulated DSC without any additional passivation layer. From Table 2, it can be seen that the simulated DSC with $TiO_2$ passivation layer has higher $J_{\text{sc}}$ compared to simulated DSC without additional layer. $J_{\text{sc}}$ is 11.649 mA/cm$^2$ for simulated DSC with additional $TiO_2$ layer as passivation layer and 11.364 mA/cm$^2$ for simulated DSC without any additional passivation layer. This higher $J_{\text{sc}}$ results in higher efficiency of DSC with additional $TiO_2$ passivation layer compared to DSC without any passivation layer due to less recombination. Meanwhile, $V_{\text{oc}}$ values of them both are close to each other. It demonstrated that the additional passivation layer can increase the performance of DSC.

*3.2. Effects of Passivation Layer Material.* The performance of simulated DSC is shown in Table 2 and also being compared with the closest experimental works. As presented in Table 2, $J_{\text{sc}}$ of simulated DSC using $TiO_2$, $Nb_2O_5$, and ZnO as passivation layer are 11.649 mA/cm$^2$, 7.952 mA/cm$^2$, and 7.972 mA/cm$^2$, respectively. These three materials are selected since they have close conduction band with $TiO_2$ as can be seen in Figure 3.

Table 2: Performance of DSC with various materials as passivation layer.

| Layer | Ref. | $J_{\text{sc}}$ (mA/cm$^2$) | $V_{\text{oc}}$ (V) | FF | Efficiency (%) |
|---|---|---|---|---|---|
| None | Simulation | 11.364 | 0.651 | 0.439 | 3.247 |
| | [15] | 11.401 | 0.654 | 0.443 | 3.301 |
| $TiO_2$ | Simulation | 11.649 | 0.694 | 0.424 | 3.428 |
| | [15] | 11.813 | 0.711 | 0.426 | 3.58 |
| $Nb_2O_5$ | Simulation | 7.952 | 0.900 | 0.518 | 3.347 |
| | [31] | 8.100 | 0.631 | 0.660 | 3.35 |
| ZnO | Simulation | 7.972 | 0.838 | 0.422 | 2.825 |
| | [32] | 7.010 | 0.654 | 0.623 | 2.86 |

It can be observed that simulated DSC with $TiO_2$ passivation layer has the higher $J_{\text{sc}}$ compared to the simulated DSC with $Nb_2O_5$ passivation layer and simulated DSC with ZnO passivation layer. This is attributed to the use of the same material of the passivation layer as the $TiO_2$ photoanode where interparticle connectivity will be very much improved with the CB at the same position in the energy level.

As can be seen in Table 2, the efficiency of simulated DSC using $TiO_2$, $Nb_2O_5$, and ZnO as passivation layer is 3.428%, 3.347%, and 2.825%, respectively, making the efficiency of the simulated DSC with $TiO_2$ passivation layer the highest. As for the simulated DSC with ZnO passivation layer, its lowest efficiency is believed to be due to the position of its CB above the CB of $TiO_2$ photoanode. The difference in the position of CB will create a boundary for electrons to be injected from dye N719 to the cathode through the passivation layer. On the other hand, the simulated DSC using $Nb_2O_5$ passivation layer shows higher efficiency compared to the simulated DSC with ZnO passivation layer but still lower one compared to the simulated DSC using $TiO_2$ passivation layer. This is due to the occurrence of recombination with the electrolyte because the CB of $Nb_2O_5$ is close to the CB of the electrolyte as shown in Figure 3.

From this simulation work, it can be predicted that, using appropriate material for the additional passivation layer in DSC, the electron loss from the photoanode to the dye through recombination process can be prevented. Besides that, it is also suggested that the material chosen as passivation layer has near or the same energy level with the photoanode in order to improve the electron mobility.

*3.3. Thickness of $TiO_2$ Passivation Layer.* Based on data of diffusion coefficient and electron lifetime from Eskandar et al. [15], related to (4) and (5), simulated recombination resistance and transport resistance were calculated. As can be seen in Figure 4, the recombination resistance reached optimum when the passivation layer thickness is 20 nm. This implies that the occurrence of recombination is low when 20 nm thickness of passivation layer is used. Furthermore, transport resistance touched the minimum when the passivation layer thickness is 20 nm which translates better electron mobility in such condition.

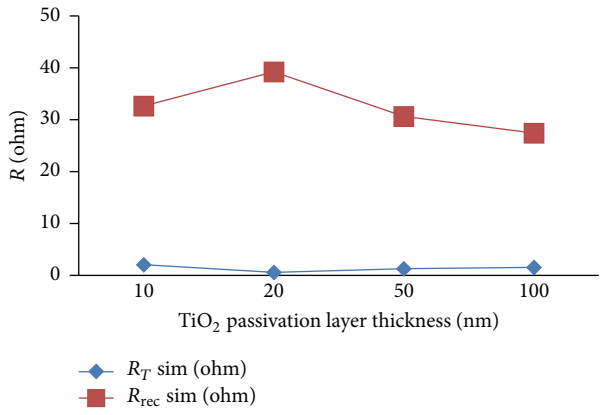


Figure 4: Resistance of simulated DSC.

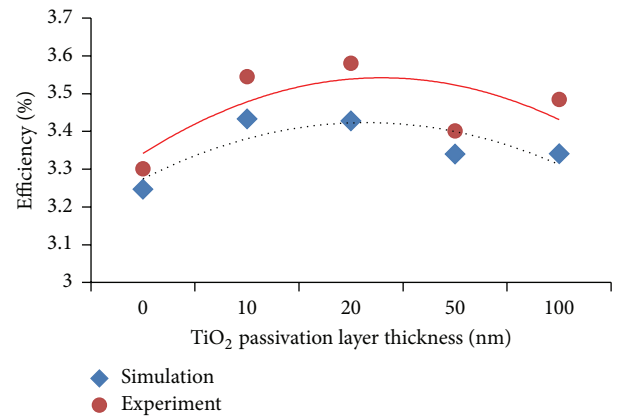


Figure 5: Efficiency of DSC with various thicknesses of $TiO_2$ passivation layer.

Table 3: Performance of DSC with various thicknesses of $TiO_2$ passivation layer.

| $TiO_2$ layer | Ref. | $J_{sc}$ (mA/cm$^2$) | $V_{oc}$ (V) | FF | Efficiency (%) |
|---|---|---|---|---|---|
| None | Simulation | 11.364 | 0.651 | 0.439 | 3.247 |
| | [15] | 11.401 | 0.654 | 0.443 | 3.301 |
| 10 nm | Simulation | 10.280 | 0.650 | 0.510 | 3.408 |
| | [15] | 10.292 | 0.669 | 0.515 | 3.545 |
| 20 nm | Simulation | 11.649 | 0.694 | 0.424 | 3.428 |
| | [15] | 11.813 | 0.711 | 0.426 | 3.58 |
| 50 nm | Simulation | 11.638 | 0.669 | 0.429 | 3.34 |
| | [15] | 11.81 | 0.667 | 0.432 | 3.401 |
| 100 nm | Simulation | 11.932 | 0.665 | 0.421 | 3.341 |
| | [15] | 12.175 | 0.664 | 0.431 | 3.485 |

The result of simulated DSC is shown in Table 3 together with the outcome of the experimental work by Eskandar et al [15]. Values of $J_{sc}$ shown in Table 3 seem to be decreasing with increasing passivation layer as the amount of electron density decreases. Result of simulated $J_{sc}$ for DSC without $TiO_2$ passivation layer is 11.364 mA/cm$^2$, whilst those with 10 nm, 20 nm, 50 nm, and 100 nm of $TiO_2$ passivation layer are 10.28 mA/cm$^2$, 11.649 mA/cm$^2$, 11.638 mA/cm$^2$, and 11.813 mA/cm$^2$, respectively. It can be seen that $J_{sc}$ is maximum for 100 nm of $TiO_2$ passivation layer. High $J_{sc}$ implies high moving electron condition where its lifetime is longer in DSC with thicker $TiO_2$ passivation layer.

Values of $V_{oc}$ for simulated DSC were found to be little fluctuating as shown in Table 3. $V_{oc}$ for DSC without $TiO_2$ passivation layer is 0.651 V, whilst, for DSC with 10, 20, 50, and 100 nm of $TiO_2$ passivation layer, the values are 0.65, 0.694, 0.669, and 0.657 V, respectively. From that simulation result, the highest $V_{oc}$ is reached when DSC is added with 20 nm $TiO_2$ passivation layer.

This 20 nm passivation layer is considered to be the optimal thickness for maximum suppression of recombination. Fill factor (FF) for DSC without $TiO_2$ passivation layer is 0.439, whilst, for DSC with 10, 20, 50, and 100 nm of $TiO_2$ passivation layer, FF are 0.51, 0.424, 0.429, and 0.421, respectively.

It is observed that the FF value is optimum when DSC is added by 20 nm $TiO_2$ passivation layer. It is the result of less occurrence of recombination because of sufficient barrier provided by 20 nm of $TiO_2$ passivation layer. This simulation result is in line with the simulation of resistance and also agreeable with the experimental result obtained by Eskandar et al., where recombination resistance peaks when passivation layer thickness is 20 nm, at a point where the transport resistance is minimal. As shown in Table 3 and Figure 5, efficiency of DSC without $TiO_2$ passivation layer is 3.247%, whilst DSCs with 10, 20, 50, and 100 nm of $TiO_2$ passivation layer are 3.408%, 3.428%, 3.34%, and 3.341%, respectively. The highest efficiency of simulated DSC is achieved by the DSC with 20 nm $TiO_2$ passivation layer.

As illustrated in Figure 5, efficiency of DSC with added $TiO_2$ passivation layer increased by 5.28% compared to the one without any passivation layer. This is attributed to the suppression of recombination by the passivation layer added in between electrolyte and TCO [34] where recombination is more prevalent. The additional $TiO_2$ passivation layer is also believed to have extended the electron lifetime for such appropriate thickness of passivation layer as also confirmed by Mohamed et al. [4]. Thicker passivation layer may lead DSC to have electron trapping which can reduce the efficiency of DSC. Both simulation and experimental result are illustrated in Figure 5 where efficiency was found to be optimum for DSC with 20 nm of $TiO_2$ passivation layer.

In Table 4, $R_T$ and $R_{Rec}$ sim are the simulation result for $R_T$ and $R_{Rec}$ whilst $R_T$ and $R_{Rec}$ exp are experimental data extracted from Eskandar et al. work [15]. The maximum error is 3.237% for RMSE, 1.1% for MBE, and 2.96% for MAE as shown in Table 4. The errors are acceptable since they are still less than 4%.

*3.4. Effects of Two-$TiO_2$ Passivation Layers.* From the previous discussion about effects of passivation layer, $TiO_2$ passivation layer, and thickness of $TiO_2$ passivation layer, simulation on DSC using two-$TiO_2$ passivation layers was

Table 4: Resistance error percentage.

| Layer thickness (nm) | 10 | 20 | 50 | 100 |
|---|---|---|---|---|
| $R_T$ sim (ohm) | 2.1 | 0.57 | 1.29 | 1.53 |
| $R_T$ exp (ohm) | 2.11 | 0.57 | 1.29 | 1.49 |
| % $R_T$ error | 0.47 | 0.11 | 0.04 | 2.8 |
| $R_{rec}$ sim (ohm) | 32.63 | 39.27 | 30.65 | 27.46 |
| $R_{rec}$ exp (ohm) | 32.04 | 39.77 | 30.5 | 27.87 |
| % $R_{rec}$ error | 1.84 | 1.25 | 0.48 | 1.46 |
| $R_{rec}/R_T$ sim (ohm) | 15.54 | 68.82 | 23.77 | 17.93 |
| $R_{rec}/R_T$ exp (ohm) | 15.2 | 69.66 | 23.72 | 18.8 |
| % $R_{rec}/R_T$ error | 2.21 | 1.2 | 0.2 | 4.63 |
| RMSE | 1.684 | 1.004 | 0.299 | 3.237 |
| MBE | 1.2 | 0.78 | 0.21 | 1.1 |
| MAE | 1.51 | 0.85 | 0.24 | 2.96 |

Table 5: Performance of simulated DSC without and with single and two $TiO_2$ passivation layers.

| $TiO_2$ layer | $J_{sc}$ (mA/cm$^2$) | $V_{oc}$ (V) | FF | Efficiency (%) |
|---|---|---|---|---|
| None | 11.364 | 0.651 | 0.439 | 3.247 |
| 20 nm | 11.649 | 0.694 | 0.424 | 3.428 |
| Two-20 nm | 11.678 | 0.692 | 0.446 | 3.604 |

also conducted. The performance of simulated DSC using two $TiO_2$ passivation layers with 20 nm thickness is presented in Table 5 in comparison with the DSC without any passivation layer.

As can be seen in Table 5, $J_{sc}$ for simulated DSC without any passivation layer, 20 nm $TiO_2$ passivation layer, and two-20 nm $TiO_2$ passivation layers are 11.364 mA/cm$^2$, 11.649 mA/cm$^2$, and 11.678 mA/cm$^2$, respectively. It can be seen that simulated DSC with two-20 nm $TiO_2$ passivation layers has the highest $J_{sc}$ among others which also indicates lower recombination occurred in simulated DSC.

$V_{oc}$ for simulated DSC without any passivation layer, 20 nm $TiO_2$ passivation layer, and two-20 nm $TiO_2$ passivation layers are 0.651 V, 0.694 V, and 0.692 V, respectively. From Table 5, it can be seen that $V_{oc}$ for simulated DSC with additional $TiO_2$ passivation layer has higher $V_{oc}$ than simulated DSC without any passivation layer. It shows that, by adding passivation layer, electron will go faster which results in higher $V_{oc}$.

The fill factors for simulated DSC without any passivation layer, 20 nm $TiO_2$ passivation layer, and two-20 nm $TiO_2$ passivation layers are 0.439, 0.424, and 0.446, respectively. The efficiencies for simulated DSC without any passivation layer, 20 nm $TiO_2$ passivation layer, and two-20 nm $TiO_2$ passivation layers are 3.247%, 3.428%, and 3.604%, respectively.

It is proven that those passivation layers suppress recombination in interface of TCO/electrolyte and $TiO_2$/electrolyte (as shown in positions A and B in Figure 1).

Lower recombination will lead to longer electron lifetime and higher electron mobility. It is confirmed that adding two-20 nm $TiO_2$ passivation layers can enhance the performance of simulated DSC.

Passivation layer is added in DSC as light scattering layer with the material the same as the photoelectrode material which is $TiO_2$. The presence of this layer can help to suppress the recombination since it is located between TCO/electrolyte and $TiO_2$/electrolyte where recombination is more prevalent. Less recombination happens in DSC which can enhance the performance of DSC.

## 4. Conclusion and Future Works

Material used and thickness of $TiO_2$ passivation layer were found to affect the performance of DSC. Simulations have been compared and validated with other experimental works that have error percentage less than 5%. Result showed that adding two-20 nm $TiO_2$ passivation layers can improve the efficiency of DSC performance by 11% as the result of less recombination, higher electron mobility, and longer electron lifetime in DSC with $TiO_2$ passivation layer.

Simulation of DSC performance showed that adding $TiO_2$ passivation layer can get DSC to reach the highest efficiency but practically, the addition of $TiO_2$ passivation layer may also be affected by the fabrication procedure. For future work, it is suggested that the fabrication of DSC should include additional $TiO_2$ passivation layer and also other optimum parameters of DSC such as 10 $\mu$m thickness of $TiO_2$ [35] and 1 M of iodide electrolyte concentration [36] to get better performance of DSC.

## Competing Interests

The authors declare that they have no competing interests.

## Acknowledgments

Supports from the Centre of Innovative Nanostructures & Nanodevices (COINN) and Graduate Assistant Scheme by Universiti Teknologi PETRONAS, Perak, Malaysia, are gratefully acknowledged.

## References

[1] M. Grätzel, "Dye-sensitized solar cells," *Journal of Photochemistry and Photobiology C: Photochemistry Reviews*, vol. 4, no. 2, pp. 145–153, 2003.

[2] M. Adachi, M. Sakamoto, J. Jiu, Y. Ogata, and S. Isoda, "Determination of parameters of electron transport in dye-sensitized solar cells using electrochemical impedance spectroscopy," *The Journal of Physical Chemistry B*, vol. 110, no. 28, pp. 13872–13880, 2006.

[3] H. Tributsch, "Function and analytical formula for nanocrystalline dye-sensitization solar cells," *Applied Physics A: Materials Science and Processing*, vol. 73, no. 3, pp. 305–316, 2001.

[4] N. M. Mohamed, M. Khatani, N. H. Hamid, A. Z. Sahmer, and S. N. A. Zaine, "Performance analysis of dye solar cell with additional $TiO_2$ layer under different light intensities," *Materials Science in Semiconductor Processing*, vol. 38, pp. 381–386, 2015.

[5] K. Zhu, E. A. Schiff, N.-G. Park, J. van de Lagemaat, and A. J. Frank, "Determining the locus for photocarrier recombination

in dye-sensitized solar cells," *Applied Physics Letters*, vol. 80, no. 4, pp. 685–687, 2002.

[6] H. Nusbaumer, J.-E. Moser, S. M. Zakeeruddin, M. K. Nazeeruddin, and M. Grätzel, "$Co^{II}(dbbip)_2^{2+}$ complex rivals tri-iodide/iodide redox mediator in dye-sensitized photovoltaic cells," *The Journal of Physical Chemistry B*, vol. 105, no. 43, pp. 10461–10464, 2001.

[7] B. Peng, G. Jungmann, C. Jäger, D. Haarer, H.-W. Schmidt, and M. Thelakkat, "Systematic investigation of the role of compact $TiO_2$ layer in solid state dye-sensitized $TiO_2$ solar cells," *Coordination Chemistry Reviews*, vol. 248, no. 13-14, pp. 1479–1489, 2004.

[8] S. Ito, P. Liska, P. Comte et al., "Control of dark current in photoelectrochemical ($TiO_2/I^-–I_3^-$) and dye-sensitized solar cells," *Chemical Communications*, no. 34, pp. 4351–4353, 2005.

[9] S. Caramori, V. Cristino, R. Boaretto, R. Argazzi, C. A. Bignozzi, and A. Di Carlo, "New components for dye-sensitized solar cells," *International Journal of Photoenergy*, vol. 2010, Article ID 458614, 16 pages, 2010.

[10] Y.-S. Jin, K.-H. Kim, W.-J. Kim, K.-U. Jang, and H.-W. Choi, "The effect of RF-sputtered $TiO_2$ passivating layer on the performance of dye sensitized solar cells," *Ceramics International*, vol. 38, no. 1, pp. S505–S509, 2012.

[11] M. F. Hossain, S. Biswas, and T. Takahashi, "The effect of sputter-deposited $TiO_2$ passivating layer on the performance of dye-sensitized solar cells based on sol–gel derived photoelectrode," *Thin Solid Films*, vol. 517, no. 3, pp. 1294–1300, 2008.

[12] S. Sodergren, A. Hagfeldt, J. Olsson, and S.-E. Lindquist, "Theoretical models for the action spectrum and the current-voltage characteristics of microporous semiconductor films in photoelectrochemical cells," *Journal of Physical Chemistry*, vol. 98, no. 21, pp. 5552–5556, 1994.

[13] R. A. Sinton and R. M. Swanson, "Recombination in highly injected silicon," *IEEE Transactions on Electron Devices*, vol. 34, no. 6, pp. 1380–1389, 1987.

[14] A. Mathew, G. M. Rao, and N. Munichandraiah, "Effect of $TiO_2$ electrode thickness on photovoltaic properties of dye sensitized solar cell based on randomly oriented Titania nanotubes," *Materials Chemistry and Physics*, vol. 127, no. 1-2, pp. 95–101, 2011.

[15] A. Eskandar, N. M. Mohamed, N. Nayan, R. A. M. Ali, S. A. A. Sharifuddin, and S. Omar, "Study on the use of $TiO_2$ passivation layer to reduce recombination losses in dye sensitized solar cells," in *Proceedings of the International Conference on Fundamental and Applied Sciences (ICFAS '12)*, Kuala Lumpur, Malaysia, June 2012.

[16] S. M. Waita, B. O. Aduda, J. M. Mwabora et al., "Electron transport and recombination in dye sensitized solar cells fabricated from obliquely sputter deposited and thermally annealed $TiO_2$ films," *Journal of Electroanalytical Chemistry*, vol. 605, no. 2, pp. 151–156, 2007.

[17] L. Han, A. Fukui, Y. Chiba et al., "Integrated dye-sensitized solar cell module with conversion efficiency of 8.2%," *Applied Physics Letters*, vol. 94, no. 1, Article ID 013305, 2009.

[18] Y. H. Jang, X. Xin, M. Byun, Y. J. Jang, Z. Lin, and D. H. Kim, "An unconventional route to high-efficiency dye-sensitized solar cells via embedding graphitic thin films into $TiO_2$ nanoparticle photoanode," *Nano Letters*, vol. 12, no. 1, pp. 479–485, 2012.

[19] M. Shanmugam, M. Farrokh Baroughi, and D. Galipeau, "High VOC dye sensitised solar cell using RF-sputtered $TiO_2$ compact layers," *Electronics Letters*, vol. 45, no. 12, pp. 648–649, 2009.

[20] S. Michael, A. D. Bates, and M. S. Green, "Silvaco ATLAS as a solar cell modeling tool," in *Proceedings of the Conference Record of the 31st IEEE Photovoltaic Specialists Conference*, pp. 719–721, January 2005.

[21] T. Daeneke, T.-H. Kwon, A. B. Holmes, N. W. Duffy, U. Bach, and L. Spiccia, "High-efficiency dye-sensitized solar cells with ferrocene-based electrolytes," *Nature Chemistry*, vol. 3, no. 3, pp. 211–215, 2011.

[22] C. Kittel, *Introduction to Solid State Physics*, John Wiley & Sons, New York, NY, USA, 6th edition, 1986.

[23] N. Fuke, A. Fukui, A. Islam et al., "Influence of $TiO_2$/electrode interface on electron transport properties in back contact dye-sensitized solar cells," *Solar Energy Materials & Solar Cells*, vol. 93, no. 6-7, pp. 720–724, 2009.

[24] J. E. Mann, S. E. Waller, D. W. Rothgeb, and C. C. Jarrold, "Study of $Nb_2O_y$ (y = 2–5) anion and neutral clusters using anion photoelectron spectroscopy and density functional theory calculations," *The Journal of Chemical Physics*, vol. 135, no. 10, Article ID 104317, 2011.

[25] H.-Y. Lee, B.-K. Wu, and M.-Y. Chern, "Schottky photodiode fabricated from hydrogen-peroxide-treated ZnO nanowires," *Applied Physics Express*, vol. 6, no. 5, Article ID 054103, 3 pages, 2013.

[26] Y. Zhao, X. Zhou, L. Ye, and S. C. Tsang, "Nanostructured $Nb_2O_5$ catalysts," *Nano Reviews*, 2012.

[27] A. V. Patil, C. G. Dighavkar, S. K. Sonawane, S. J. Patil, R. Y. Borse, and J. Optoelectron, "Effect of firing temperature on electrical and structural characteristics of screen printed ZnO thick films," *Journal of Optoelectronics and Biomedical Materials*, vol. 1, no. 2, pp. 226–233, 2009.

[28] O. Tonomura, T. Sekiguchi, N. Inada, T. Hamada, H. Miki, and K. Torii, "Band Engineering of Rutile $TiO_2$ by Cobalt Doping in Ru/Rutile-$TiO_2$/Ru Capacitor aiming 40-nm DRAM and Beyond, Silicon Nitride, Silicon Dioxide, and Emerging Dielectrics 10," vol. 743, The Electrochemical Society, 2009.

[29] K. Knapas, A. Rahtu, and M. Ritala, "Etching of $Nb_2O_5$ thin films by $NbCl_5$," *Chemical Vapor Deposition*, vol. 15, no. 10–12, pp. 269–273, 2009.

[30] N. H. Langton and D. Matthews, "The dielectric constant of zinc oxide over a range of frequencies," *British Journal of Applied Physics*, vol. 9, no. 11, article 453, 1958.

[31] J. Xia, N. Masaki, K. Jiang, and S. Yanagida, "Sputtered $Nb_2O_5$ as a novel blocking layer at conducting glass/$TiO_2$ interfaces in dye-sensitized ionic liquid solar cells," *Journal of Physical Chemistry C*, vol. 111, no. 22, pp. 8092–8097, 2007.

[32] F. Al-Juaid and A. Merazga, "Increasing dye-sensitized solar cell efficiency by ZnO spin-coating of the $TiO_2$ electrode: effect of ZnO amount," *Energy and Power Engineering*, vol. 5, no. 10, pp. 591–595, 2013.

[33] T. Goudon, V. Miljanović, and C. Schmeiser, "On the Shockley-Read-Hall model: generation-recombination in semiconductors," *SIAM Journal on Applied Mathematics*, vol. 67, no. 4, pp. 1183–1201, 2007.

[34] Y. S. Jin and H. W. Choi, "The effect of different Tio2 passivating layers on the photovoltaic performance of dye-sensitized solar cells," *Journal of Ceramic Processing Research*, vol. 13, no. 2, pp. 178–183, 2012.

[35] U. Y. Oktiawati, N. M. Mohamed, and Z. A. Burhanudin, "Effects of $TiO_2$ electrode thickness on the performance of dye solar cell by simulation," in *Proceedings of the IEEE Regional Symposium on Micro and Nano Electronics (RSM '13)*, pp. 406–409, Langkawi, Malaysia, September 2013.

[36] U. Y. Oktiawati, N. M. Mohamed, and Z. A. Burhanudin, "Simulation of the effects of electrolyte concentration on dye solar cell performance," in *Proceedings of the 5th International Conference on Intelligent and Advanced Systems (ICIAS '14)*, IEEE, Kuala Lumpur, Malaysia, June 2014.